

Department of Physics and Astronomy

University of Heidelberg

Bachelor thesis

in Physics

submitted by

Bernd Kristof Mumme

born in Krefeld

2020

**Towards an inclusive search
for heavy neutral leptons
at the LHCb experiment**

This Bachelor thesis has been carried out by Bernd Kristof Mumme

at the

Physikalisches Institut

under the supervision of

Prof. Dr. Stephanie Hansmann-Menzemer

Auf dem Weg zu einer inklusiven Suche nach Schweren Neutralen Leptonen am LHCb-Experiment:

Diese Arbeit setzt es sich zum Ziel, Monte-Carlo Daten zu simulieren und eine vorläufige Machbarkeitsstudie für die Suche nach Schweren Neutralen Leptonen (HNLs), die in B -Meson-Zerfällen am LHCb produziert werden. Während die Suche nach HNLs in der exklusiven Produktion und Zerfall ($B^+ \rightarrow \mu^+(N \rightarrow \mu^+\pi^-)$) durchgeführt wurden, hoffen wir, mit unserer neuartigen Herangehensweise, die vollständig inklusive Produktion und Zerfall ($B \rightarrow \mu X(N \rightarrow X\mu\pi)$) zu betrachten, die Sensitivität von LHCb für die Suche nach HNLs stark zu verbessern.

Monte-Carlo-Simulation wird für fünf verschiedene HNL Massenpunkte zwischen (1.6 – 5.5) GeV, drei verschiedene Lebensdauern von (10, 100 and 1000) ps, alle B -Meson-Zerfälle und sowohl Myonen-Paare mit gleichen als auch ungleichen Vorzeichen vorbereitet und produziert. Diese Proben werden benutzt, um die inklusive Suche voranzutreiben und die Detektorakzeptanz zu modellieren. Außerdem wird eine vorläufige Analyse einer kleinen Menge der produzierten Simulation (drei B^0 -Datensätze) durchgeführt, um die Integrität der produzierten Simulation zu verifizieren und eine Abschätzung der Machbarkeit der Suche nach HNLs am LHCb mit dieser Methode zu geben.

Towards an inclusive search for Heavy Neutral Leptons at the LHCb experiment:

This thesis aims to set up Monte Carlo simulation and to provide a preliminary feasibility analysis for the search for Heavy Neutral Leptons produced in B hadron decays at LHCb. While studies on the exclusive production and decay channel ($B^+ \rightarrow \mu^+(N \rightarrow \mu^+\pi^-)$) have been conducted, we hope that this new approach of a fully inclusive production and decay ($B \rightarrow \mu X(N \rightarrow X\mu\pi)$) allows us to significantly improve the sensitivity of LHCb to Heavy Neutral Lepton searches.

Monte Carlo simulation is prepared for five different Heavy Neutral Lepton mass points between (1.6 – 5.5) GeV and three different lifetimes at (10, 100 and 100) ps, all B hadron production modes and same sign as well as opposite sign muons in the decay. The simulated samples be used to design the inclusive search and model the detector acceptance to the signal. Furthermore a preliminary analysis on a subset of three B^0 samples is conducted to verify the integrity of the produced Monte Carlo data and give an estimate of the feasibility of the Heavy Neutral Lepton search with this method.

Contents

I	Introduction	3
1	Motivation	4
2	LHCb	5
2.1	Tracking System	5
2.2	Particle Identification System	6
2.3	Trigger and Analysis Framework	6
3	The Standard Model of Particle Physics	8
4	Heavy Neutral Leptons	10
II	Monte Carlo Production	11
5	Decay Structure	12
5.1	Exclusive Production and Exclusive Decay	14
5.2	Inclusive Production and Exclusive Decay	14
5.3	Inclusive Production and Inclusive Decay	15
6	Simulation	18
III	Search strategy	20
7	Selection Criteria	21
8	Corrected Mass Technique	24
9	Event rate ratio	30
IV	Conclusion	32
10	Comments and Outlook	33

V	Appendix	34
A	Additional mass plots	35
B	Additional chi2 plots	36
C	Lists	37
C.1	List of Figures	37
C.2	List of Tables	38
D	Bibliography	39

Part I

Introduction

1 Motivation

The Standard Model (SM) describes the world of particles to the best of today's knowledge. However, it cannot be a complete theory of the universe, because it leaves several questions open, like for example the Baryonic Asymmetry in the Universe (BAU). Thus, searches for beyond SM physics phenomena are one of the major priorities of the High Energy Physics community. LHCb is one of the four experiments at the Large Hadron Collider (LHC) at the Conseil Européenne pour la Recherche Nucléaire (CERN), which is dedicated to new physics searches. The main target of LHCb are indirect searches in quantum loops in B and D hadron decays.

One promising signature to look for are Heavy Neutral Leptons (HNLs), which could explain several of the open questions of the SM. A first limit on HNL has been determined by LHCb exploiting the exclusive channel of the beauty meson decay $B^+ \rightarrow \mu^+(N \rightarrow \mu^+\pi^-)$, where N is an HNL. This approach lies well within the limits explored by other experiments before. This thesis studies the possibility to extend this approach to the inclusive channels $B \rightarrow X\mu(N \rightarrow X\mu\pi)$. The inclusive approach takes HNL from all B hadron decays into account and considers all HNL decay modes including a muon and a pion. This method has the potential to significantly improve the sensitivity of the HNL search at LHCb.

The main goal of this thesis is to set up the automated Monte Carlo (MC) simulation to obtain all samples needed for this sensitivity study and an initial validation of a subset of them. These samples cover five mass points in the range of (1.6-5.5) GeV, three different HNL lifetimes at (10, 100 and 1000) ps, all B hadrons as production modes and HNL decays with a pair of same sign as well as opposite sign muons.

This thesis first introduces the concept of HNLs and why they are interesting. Then an overview of the LHCb experiment and its analysis framework is given. Afterwards the specific decays, which will be simulated, are presented. In the last part we will introduce a technique to reconstruct the HNL mass in the inclusive decay channels and provide a preliminary analysis on a subset of the generated Monte Carlo data. Finally we will summarise and give an outlook.

2 LHCb

LHCb is one of the four main experiments at the Large Hadron Collider (LHC), a circular proton collider at CERN, a laboratory for nuclear research located in Geneva, Switzerland. It has a circumference of 27 km and is the most powerful circular collider ever constructed. LHCb has had two runs so far, with an integrated luminosity of 3 fb^{-1} at 7.8 TeV collision energy in Run 1 (2009-2013) and 6 fb^{-1} at 13 TeV in Run 2 (2015 – 2018). Currently under shutdown, it is being prepared for Run 3, scheduled to start 2022 with a luminosity five times as high as before.

The LHCb detector [3] is a single-arm forward spectrometer covering the pseudorapidity range $2 < \eta < 5$, designed for precision measurements of charm and beauty hadrons in the search for New Physics.

2.1 Tracking System

The LHCb detector implements different systems for track reconstruction: the Vertex LOcator (VELO) and the tracking stations. Figure 2.1 shows a side view of the detector. The VELO, seen on the very left, is used to obtain precise track coordinates of charged particles close to the interaction point. This is especially useful to detect displaced secondary vertices that are frequent in beauty and charm decays.

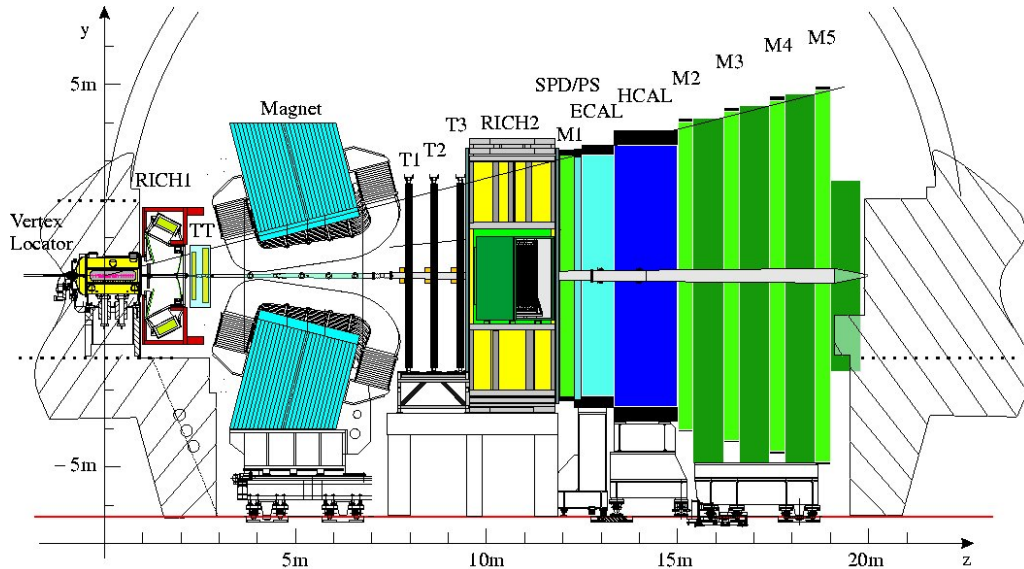


Figure 2.1: Schematic of the LHCb detector [3].

The Trigger Tracker (TT) upstream of the magnet and the three tracking stations (T1–T3) downstream of the magnet provide further information for track reconstruction. The TT station gives a first approximation of the particle momentum, while the three tracking stations downstream provide more precise measurements.

2.2 Particle Identification System

Particle IDentification (PID) in LHCb is done by the RIng CHerenkov imaging detectors (RICH), a calorimeter system consisting of an Electromagnetic CALorimeter (ECAL) and a Hadronic CALorimeter (HCAL). Additionally, there are two further detectors, the PreShower detector (PS) and a Scintillating Pad Detector (SPD).

RICH1 is used to identify low momentum particles and therefore placed directly after the VELO and upstream of the magnet. RICH2 on the other hand is used to identify higher momentum particles and therefore placed downstream of the tracking stations. They are used for hadron separation. Downstream of RICH2 we have the calorimeters that are used to identify electrons and neutral particles.

Especially important for the data simulated and analysed in this thesis are the Muon chambers (M1–M5), because we encounter muons in all final states. M1 is placed upstream of the calorimeters and used to improve the p_T measurement for the online trigger. M2–M5 are located downstream of the calorimeters.

2.3 Trigger and Analysis Framework

The LHCb detector receives about 40 million proton–proton collisions per second, which results in a huge amount of data, roughly 1 TB per second. Because we cannot physically store all of this data, LHCb implements three trigger stages, the Level Zero Trigger (L0), which is implemented in hardware, and two High Level Triggers (HLT1 and HLT2), that are implemented in software, to filter the data and keep

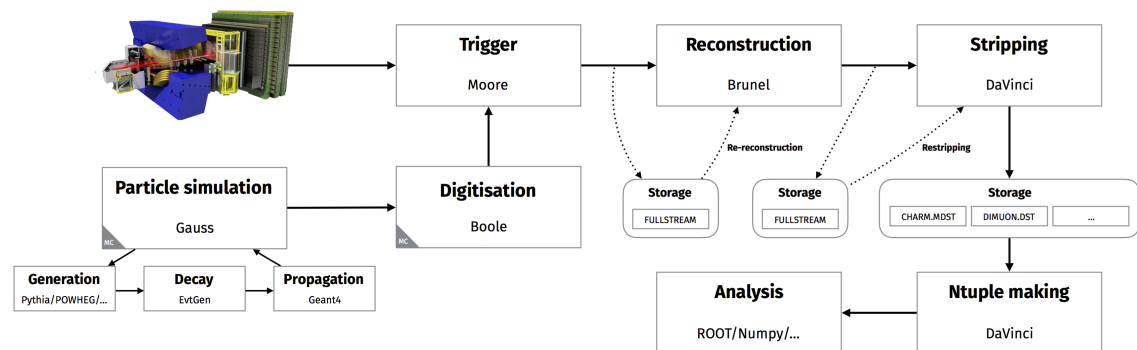


Figure 2.2: Data flow at LHCb [8].

only events that contain interesting information. The software stage of the trigger is implemented in MOORE. This and the further data flow are shown in Figure 2.2. Particle trajectories, calorimeter clusters and muon and RICH signals are reconstructed offline in BRUNEL. Afterwards, this reconstructed data is further filtered through sets of selections called stripping, which is done in DAVINCI.

To test certain decays before looking for their signatures in real data, events are simulated, we also call this Monte Carlo simulation. The particle simulation in the LHCb data flow is handled by GAUSS. GAUSS is responsible for supervising the simulation process. First, it calls a Monte Carlo generator like PYTHIA [12, 13], then it calls EVTGEN [11], which simulates the decays of the long-lived particles, such as B or D hadrons. GEANT4 is then used to simulate the propagation and interaction of particles through and with the detector. The simulated events are then converted to signals that mimic real data by the BOOLE application, so that the Monte Carlo events can also be processed by the trigger, reconstruction and stripping just like data from the experiments. One of the goals of this thesis is to set GAUSS up to simulate events of HNL production and decays.

3 The Standard Model of Particle Physics

The Standard Model (SM) of particle physics is currently the most accurate model we have to describe the interactions of subatomic particles through three of the four fundamental forces of nature, electromagnetism, the weak and the strong interaction.¹ Each of these three forces is described by a field in Quantum Field Theory (QFT) and corresponds to the exchange of particles called bosons.

The SM is comprised of six quarks and six leptons. Three of the leptons are charged and three of them carry no charge. Furthermore, the SM contains the bosons that mediate the corresponding forces, the gluon for the strong interaction, the photon for the electromagnetic interaction, and the W/Z bosons for the weak interaction. The most recent addition to the SM is the Higgs Boson, which allows particles to

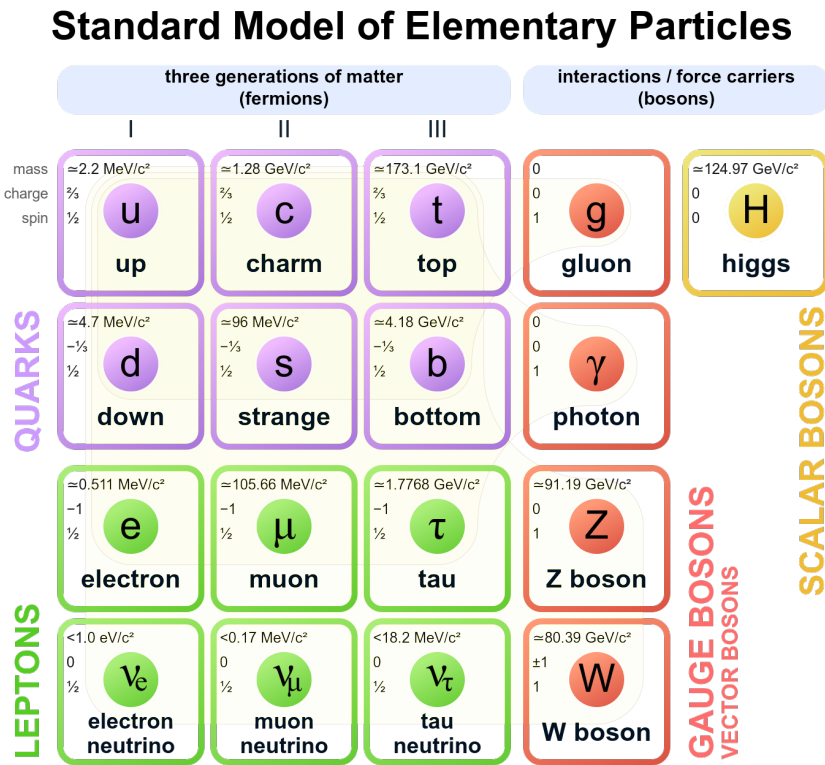


Figure 3.1: Elementary particles in the SM [10].

¹The fourth fundamental force is gravity. As far as we know, gravity is best described by General Relativity (GR), which has yet to be unified with the Standard Model.

have mass. Its experimental discovery completes the SM as seen in Figure 3.1.

Any particle comprised of two or more quarks is called a hadron, and we differentiate between baryons and mesons. Baryons consist of an odd number of quarks (mostly three), while mesons consist of an even number of quarks (mostly a quark antiquark pair). Since we will look at B meson decays, our decay products will only consist of other mesons and leptons. Table 3.1 gives an overview over the mesons that occur in the inclusive decays introduced later in this thesis and lists their basic properties.

Table 3.1: Different mesons that appear in beauty decays, their quark content and mass as well as mean lifetimes (charge conjugates are implied)[15].

Particle name	Symbol	Quark content	Mass [MeV]	Mean lifetime [s]
B meson	B^+	$u\bar{b}$	5279.2	1.6×10^{-12}
B meson	B^0	$d\bar{b}$	5279.5	1.5×10^{-12}
Strange B meson	B_s^0	$s\bar{b}$	5366.3	1.5×10^{-12}
Charmed B meson	B_c^+	$c\bar{b}$	6276.0	4.6×10^{-13}
Pion	π^+	$u\bar{d}$	139.6	2.6×10^{-8}
Pion	π^0	$u\bar{u}/d\bar{d}$	135.0	8.4×10^{-17}
Rho meson	ρ^+	$u\bar{d}$	775.4	4.5×10^{-24}
Rho meson	ρ^0	$u\bar{u}/d\bar{d}$	775.5	4.5×10^{-24}
D meson	D^+	$c\bar{d}$	1869.6	1.0×10^{-12}
D meson	D^0	$c\bar{u}$	1864.8	4.1×10^{-13}
D meson	D^{*+}	$c\bar{d}$	2010.3	6.9×10^{-21}
D meson	D^{*0}	$c\bar{u}$	2007.0	3.1×10^{-22}
Strange D meson	D^{*+}	$c\bar{s}$	1968.5	5.0×10^{-13}
Strange D meson	D_s^{*+}	$c\bar{s}$	2112.3	3.4×10^{-22}

For this thesis, we will focus on neutrinos, very light particles that, because they do not carry a charge, only interact with the other particles of the Standard Model via the weak interaction, which makes them very hard to detect. While the SM is the most tested theory in physics, it fails to explain some fundamental observations, like solar and atmospheric neutrino oscillations, Baryonic Asymmetry in the Universe (BAU) and Dark Matter (DM). The addition of sterile right-handed neutrinos could, with some constraints, solve all three of those [6].

4 Heavy Neutral Leptons

An extension of the SM that could solve the three main problems mentioned before could be the compact Neutrino Minimal Standard Model (ν MSM)[4]. It requires the addition of new sterile neutrinos N , also called Heavy Neutral Leptons (HNLs). The theory behind HNLs is summarised very well in [5]. HNLs are singlets with respect to the SM gauge group with gauge charges of zero. The HNL couples with the SM fields the same as SM neutrinos as shown in Equation 4.1.

$$\begin{aligned} \mathcal{L}_{\text{HNL},int} = & \frac{G_F}{2\sqrt{2}} W_\mu^+ \bar{N}^c \sum_\alpha U_{\alpha N}^* \gamma^\mu (1 - \gamma_5) \ell_\alpha^- \\ & + \frac{G_F}{4 \cos(\theta_W)} Z_\mu \bar{N}^c \sum_\alpha U_{\alpha N}^* \gamma^\mu (1 - \gamma_5) \nu_\alpha + h.c., \end{aligned} \quad (4.1)$$

We see that there are two parts of the equation, the interaction of the HNL with charged leptons (ℓ_α) via a W boson, and the interactions with uncharged leptons (neutrinos ν_α) via a Z boson. The Fermi constant G_F and the Weinberg angle θ_W describe the strength of the coupling, \bar{N}^c denotes the HNL, $U_{\alpha N}^*$ is the mixing angle, and γ^μ and γ_5 are the Dirac matrices. In both terms of the Lagrangian, we sum over the three lepton families ($\alpha = e, \mu, \tau$).

This coupling is strongly suppressed by the small mixing angles $U_{\alpha N}$, where again $\alpha = e, \mu, \tau$. The mixing probability is given by the square of this matrix, $U_{\alpha N}^2$.

The three important variables for this analysis will be the lifetime τ , $U_{\alpha N}$ and the HNL mass m_{HNL} . We can calculate each of them from the other two, as mentioned in [5]. The smaller the mixing angle $U_{\alpha N}$, the larger is the lifetime, and the smaller the HNL mass, the larger the lifetime as well.

In the LHCb experiment we will be looking at the mixing of HNLs with muons specifically, so we will be studying $U_{\mu N}$ in correlation with the HNL mass. In practice, we will want to simulate HNLs at different mass points and lifetimes, study the signal and determine the reconstruction and selection efficiency and background contributions. This will give an estimate of the feasibility of such a search in data from the experiment. Concluding that the search is feasible in a certain region of the $U_{\mu N}$ mass space we will call being sensitive to said region. Searching in actual data from the experiment we may either find a particle, or if we do not find one, conclude with a certain confidence that we can exclude the region we searched in from further searches.

Part II

Monte Carlo Production

5 Decay Structure

In this thesis we will study the HNLs produced in B meson decays. B mesons decay via the weak interaction, which entails the radiation of a W boson, which in turn can decay to a charged lepton and a neutrino, in this case the HNL, as shown in Figure 5.1.

First, we will distinguish between exclusive production and inclusive production of the HNL. The exclusive production is defined in Figure 5.1, where the B meson decays via the weak interaction radiating a W boson, which then decays further. Specifically, the decay channel we will be defining as exclusive is $B^+ \rightarrow \mu^+(N \rightarrow \mu^+\pi^-)$ (and its charge conjugate).

In the inclusive production as shown in Figure 5.2, we will now allow any type of B meson to produce an HNL, but ultimately ignore the additional hadronised final states that come with it. The entire selection of inclusive B decays we will simulate Monte Carlo data for is shown in Figure 5.4a.

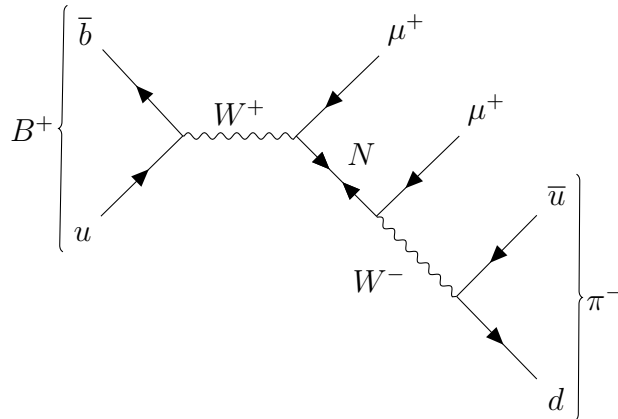


Figure 5.1: Feynman diagram of the exclusive production and exclusive decay of HNL. An initial B^+ meson decays via the weak interaction radiating a W boson, which decays into a lepton and an HNL. The HNL then decays again into a muon and a pion.

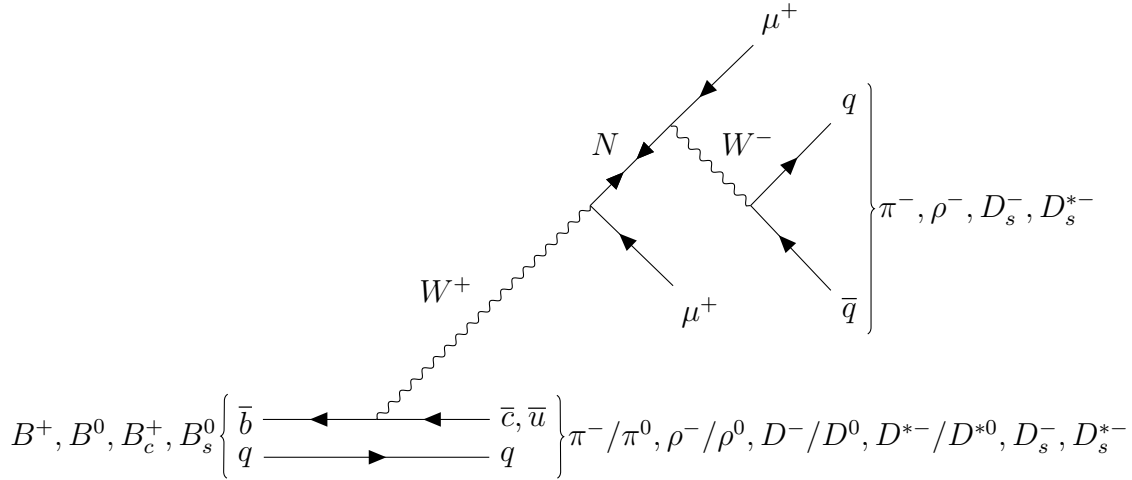


Figure 5.2: Feynman diagram of the inclusive production and inclusive decay of HNL. Any type of B meson decays weakly, hadronising in a different meson, while the W boson decays into an HNL and a lepton. The HNL is allowed to decay to a muon and any meson with a pion in the final state.

The HNL then decays, unlike the SM neutrino, into a charged lepton and a virtual W boson, which again decays into some quark-quark pair or a charged lepton and a neutrino. The neutral decay via a Z boson can also happen, but is not prevalent for $m_{\text{HNL}} < 5$ GeV and much harder to detect, because it contains a second neutrino in the production chain instead of a charged lepton. We want to scan the $U_{\alpha N}$ -mass space for the occurrence of an HNL. Specifically, in LHCb, we are looking at $U_{\mu N}$, and only considering final states that contain muons.

In the exclusive production as defined in Figure 5.1, we reconstruct the B meson from the $\pi\mu\mu$ invariant mass and the HNL from the $\mu\pi$ invariant mass. In the inclusive production modes, we lose the ability to reconstruct the B meson candidates fully, since we ignore the hadronised final states relating to the B meson.

We will further distinguish between exclusive and inclusive decay of the HNL. Exclusive decay of the HNL means that we only consider final states with one muon and one pion ($N \rightarrow \mu\pi$). The HNL decays into a lepton and a W boson, and we only consider the final states where the W boson hadronises as a pion. Here, we can reconstruct the HNL candidate fully using the $\mu\pi$ invariant mass. In the inclusive decay of the HNL, we still reconstruct the HNL candidate as $\mu\pi$, but include all final states that include at least one pion. This means that we underestimate the HNL mass and need to correct for the missing particles of the heavier hadronisations, a technique for this is introduced in chapter 8.

5.1 Exclusive Production and Exclusive Decay

The earliest result of an LHCb search for HNL's was by the LHCb collaboration in [1], which looked at the exclusive channel ($B^- \rightarrow \mu^- (N \rightarrow \pi^+ \mu^-)$) and searched for peaks in the $\pi^+ \mu^-$ as well as in the $\pi^+ \mu^- \mu^-$ invariant mass. This analysis was done on same sign muons, because that decay channel has a significantly lower background than the one with opposite sign muons, since B meson decays with same sign muons are strongly suppressed in the standard model. No signal was found and the analysis allowed to exclude the values for $U_{\mu N}^2$ and HNL mass shown in Figure 5.3.

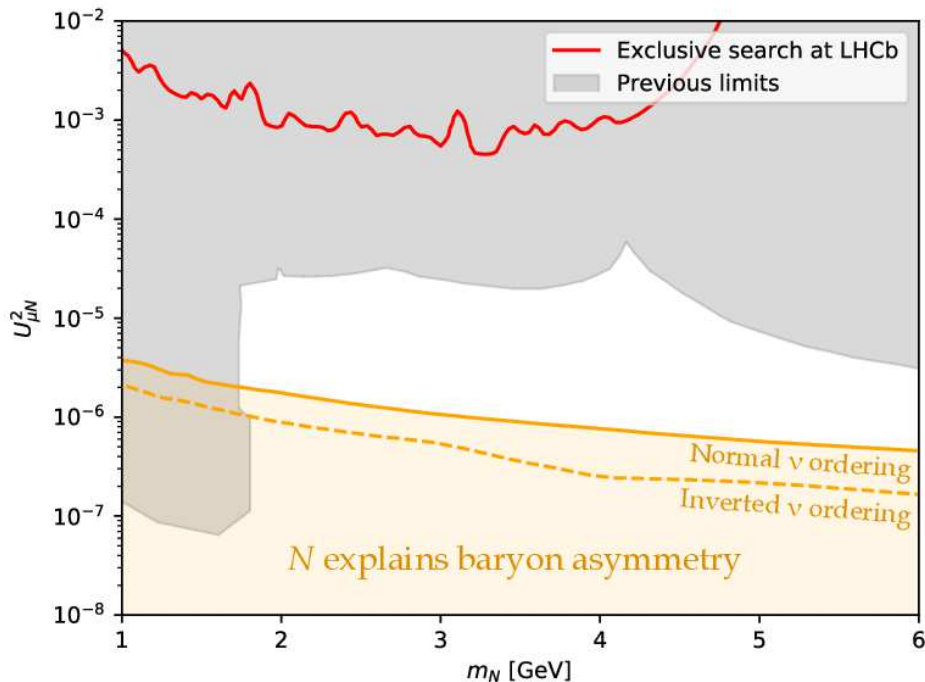


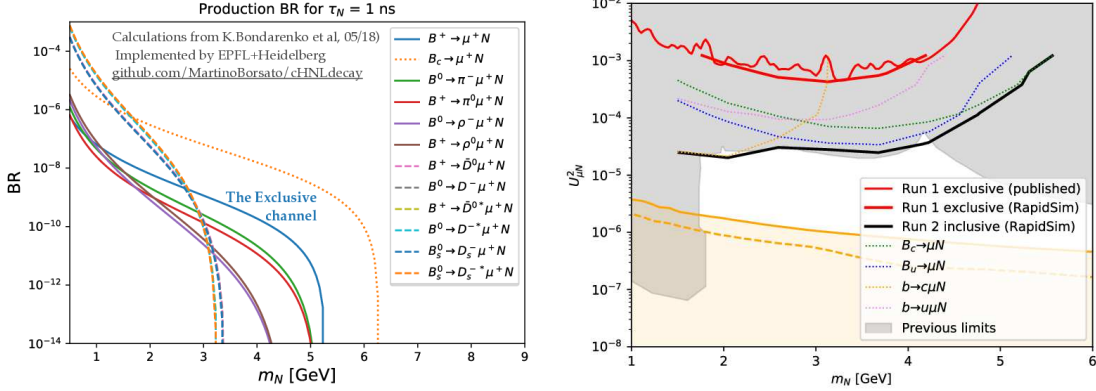
Figure 5.3: Parameter regions of the HNL search for exclusive production and decay excluded at a 90 % confidence level, showing HNL mass [GeV] against the mixing probability $U_{\mu N}^2$. The red line shows the exclusion limit for this analysis, the grey shaded area shows limits determined by other experiments previously, and the yellow shaded area shows the region of the $U_{\mu N}^2$ -mass space where the HNL would explain BAU [4].

The advantage of this strategy are clear peaks in the $\pi^+ \mu^-$ and $\pi^+ \mu^- \mu^-$ invariant masses, but as a tradeoff, statistics are low.

5.2 Inclusive Production and Exclusive Decay

The next idea was to leave the HNL decay exclusive, but include a lot of other B meson decay channels in the search, allowing $B \rightarrow X \mu^- N (\rightarrow \pi^+ \mu^-)$. Still, this

analysis is designed to be done on same sign muons. Since we ignore the particles X above, we lose the peak in the $\pi\mu\mu$ invariant mass and cannot reconstruct the B meson candidate anymore.



(a) B branching ratios for all inclusive channels, (b) Inclusive production and exclusive decay, plotted against the HNL mass, showing preliminary simulation of the sensitivity with inclusive production and exclusive decay of HNLs.

Figure 5.4: B branching ratios and inclusive production sensitivity.

As can be seen in Figure 5.4a, including these other production channels gives a lot of extra statistics, especially in the lower mass region below 3000 MeV. Simulating the inclusive production with a fast parametric simulation of the LHCb experiment (RAPIDSIM [9]) gave an estimate for sensitivity at the limits of previous experiments. Analysis for this mode is currently being carried out by a collaboration between the École polytechnique fédérale de Lausanne (EPFL) and Heidelberg University, for which the Monte Carlo data produced in the scope of this thesis is essential for studying the inclusive B decay channels.

5.3 Inclusive Production and Inclusive Decay

The last idea is to look at the inclusive decay as well. Until now, we have only allowed the B meson to decay to anything including a muon in the final state, while the HNL was forced to decay to a muon and a pion ($N \rightarrow \mu\pi$). Now we also want to allow the HNL to decay to other hadrons that contain a pion in the final state, which will happen via the hadronic decay mode as shown in Figure 5.2. The resulting production and decay will then look like $B \rightarrow X\mu^- N (\rightarrow X\mu^-)$.

The branching ratios of the HNL decay are shown in Figure 5.5. As we see, the exclusive channel does not contribute a significant amount to the larger mass states, where we get more contributions from the heavier particles. We want to simulate HNLs up to 5500 MeV this way, which should give us further gain in the sensitivity,

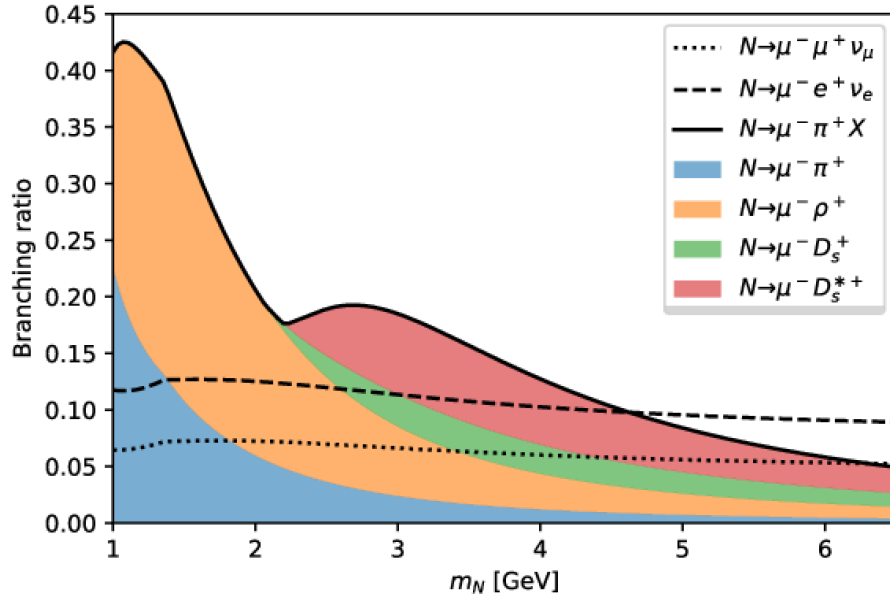


Figure 5.5: Branching ratios of the different HNL decay modes. We will not be studying the $N \rightarrow \mu^- \mu^+ \nu_\mu$ and $N \rightarrow \mu^- e^+ \nu_e$, since they are hard to detect, but it is obvious that the inclusive channel gives us a lot more statistics, especially in the higher mass regions.

an improvement over Figure 5.4b. Since we are being inclusive, we will also simulate MC for the channels with opposite sign muons and study the background contributions to figure out whether or not a search in data would be feasible. Table 5.1 summarises the results from above. In the following we will discuss why the strategy of inclusive production and inclusive decay offers new opportunities.

Table 5.1: Different production and decay modes for the HNL in beauty decays.

Exclusive prod + decay	Inclusive production	Inclusive prod + decay
$B^- \rightarrow \mu^- N (\rightarrow \pi^+ \mu^-)$	$B^- \rightarrow X \mu^- N (\rightarrow \pi^+ \mu^-)$	$B^- \rightarrow X \mu^- N (\rightarrow \mu^- X)$
Displaced $\pi^+ \mu^-$	Displaced $\pi^+ \mu^-$	Displaced $\pi^+ \mu^-$
Peak in $\pi^+ \mu^- \mu^-$ mass	Peak in $\pi^+ \mu^- \mu^-$ mass	Peak in $\pi^+ \mu^- \mu^-$ mass
Peak in $\pi^+ \mu^-$ mass	Peak in $\pi^+ \mu^-$ mass	Peak in $\pi^+ \mu^-$ mass
Same sign muons	Same sign muons	Same sign muons (and opposite sign)

The main difference between these channels is that for the inclusive decays we lose the peak in the $\pi^+\mu^-\mu^-$ mass and then with the inclusive production and decay also the peak in the $\pi^+\mu^-$ mass. This means that we have to reconstruct the HNL mass using a partial reconstruction as described in chapter 8. In return, using the inclusive production gives us a large improvement in coverage of the $U_{\mu N}^2$ -mass space, at the loss of some efficiency, so the hope for this analysis is to further improve the sensitivity by using not only inclusive production but also the inclusive decay. As can be seen in Figure 5.4a, we gain a lot of coverage of the lower mass space, up to higher branching ratios, and most of all, more statistics through this inclusive approach. In the decay, we also gain a significant amount of statistics, as can be seen in Figure 5.5. In the following, we describe the generation of Monte Carlo simulation of the inclusive events as described above, and give a preliminary analysis of the produced Monte Carlo data.

6 Simulation

The main part of this thesis is the setup to simulate Monte Carlo data for all the inclusive channels shown in Figure 5.4a and Figure 5.5 at LHCb. To do this, I use a program written by Fabian Thiele [14], which calculates the branching ratios. Then I procedurally generate the information at different lifetimes and masspoints of the HNL needed by GAUSS to be able to study the decays most efficiently.

Table 6.1: B mesons, muon signs, HNL masspoints and HNL lifetimes we want to simulate Monte Carlo data at.

B meson	B^+, B^0, B_c^+, B_s^0
μ Sign	Same Sign (SS, $\mu^+\mu^+$) and Opposite Sign (OS, $\mu^+\mu^-$)
HNL Masspoints	(1600, 2000, 3000, 4000, 5000 and 5500) MeV
Lifetimes	(10, 100 and 1000) ps

While the requirements listed in Table 6.1 would make for a total of 144 different production and decay modes, some of them are unphysical and have to be discarded in the process. For example, as can be seen in Figure 5.4a, the two B_s^0 channels will have non-zero branching ratios only for HNL masses below $m_{\text{HNL}} = 4000$ MeV, and higher mass points will therefore have to be discarded. In addition, it is important to distinguish between the neutral B meson decays and the charged B mesons, as they have to be set up slightly differently in software.

Writing an automated process to calculate all branching ratios, check if they are physical, discard unphysical conditions and set up simulation for all others was the main work of this thesis. This process produces a total of 114 simulation points for all different production and decay channels. They are tested locally and small test samples of 20 events are produced.

The samples are generated with PYTHIA [12, 13] for the production of the B meson, and the decay of the hadrons is forced to the HNL channels with EVTGEN, while neglecting polarisation (PHSP). The B_c^+ decays use the special BCVEGPy production mode [7].

Then we request a small sample of three B^0 lifetimes for a preliminary test, which the analysis of this thesis is based on as well. These samples are B^0 , SS, 3000 MeV for (10, 100 and 1000) ps respectively.

At the time of writing, larger Monte Carlo data samples for all 114 simulation points is produced, however, this thesis will only provide preliminary analysis of a subset of three of these simulation points.

A sample configuration will be shown below, specifically for one of the simulation points we will analyse later, B^0 , SS, 3000 MeV and 100 ps.

Table 6.2: B^0 decay branching ratios for SS muons, $m_{\text{HNL}} = 3000$ MeV and $\tau_{\text{HNL}} = 100$ ps.

Branching ratio	B Decay Products		
0.4906	HNL	μ^\pm	π^\mp
0.0477	HNL	μ^\pm	ρ^\mp
0.2903	HNL	μ^\pm	D^\mp
0.1714	HNL	μ^\pm	$D^{*\mp}$

We can see in Table 6.2 that the $\pi\mu$ channel is prevalent, but especially the hadronic channels have quite a large contribution to the overall event rate as well.

Table 6.3: HNL decay branching ratios for SS muons, $m_{\text{HNL}} = 3000$ MeV and $\tau_{\text{HNL}} = 100$ ps.

Branching ratio	HNL Decay Products	
0.1297	μ^\pm	π^\mp
0.3323	μ^\pm	ρ^\mp
0.1536	μ^\pm	D_s^\mp
0.3844	μ^\pm	$D_s^{*\mp}$

For the HNL as seen in Table 6.3, in this specific case, the exclusive channel only makes up 13% of the total branching ratio, with the D_s^{*+} and ρ channels contributing over 30% each, so we gain a lot of events here.

Part III

Search strategy

7 Selection Criteria

We will be using a selection process developed by the analysis team at EPFL and Heidelberg for the inclusive production of the HNL, but not the inclusive decay. In the selection process, we are looking for a final state of $\pi\mu\mu$, where the π and one of the muons come from the HNL in the exclusive decay, while in the inclusive decay we allow the π to be product of a further decay product of the HNL. The second μ originates from the B meson that starts the decay, so it is displaced with respect to the $\pi\mu$.

Table 7.1: L0 trigger selection.

Trigger decision	Cut	Value
L0DiMuon	$p_T(\mu^+)$ and $p_T(\mu^-)$	$\gtrsim 1.5$ GeV
	nSPD	< 900
L0Muon	$p_T(\mu^+)$ or $p_T(\mu^-)$	$\gtrsim 1.8$ GeV
	nSPD	< 600

At the first level (L0), described in Table 7.1, we trigger using the transverse momentum of either one of the muons or both of them, meaning any candidate has to pass either L0DiMuon or L0Muon, and on the number of track hits in the Scintillating Pad Detector (SPD), to lower computation time for higher level triggers and filter out busy events.

Table 7.2: HLT1 trigger selection (Hlt1TrackMuon).

Cut	Value
$p(\mu)$	> 6000 MeV
$p_T(\mu)$	> 1100 MeV
μ Track χ^2/dof	< 3
μ Ghost probability	< 0.2
μ Minimum IP- χ^2 w.r.t. PV	> 35

In the software level online selection we place stronger requirements. The HLT1

trigger as shown in Table 7.2 requires one muon with a large momentum, a good track quality (small ghost probability, small track χ^2), and a high impact parameter (IP). This impact parameter is defined as the closest distance between the extrapolated track and the position of the primary vertex (PV). We want the IP to be large for the muons to make sure that they are coming from a displaced decay (like in our case the B or HNL).

Table 7.3: HLT2 trigger selection (Hlt2MajoranaBLambdaMu).

Cut	Value
m_B	$\in \{1500, 6500\}$ MeV
B Vertex χ^2/dof	< 4
B DIRA _{PV}	> 0.99
m_N	> 1500 MeV
p_{TN}	> 700 MeV
N χ^2 -separation from PV	> 100
N Vertex χ^2/dof	< 10
p_π	> 2000 MeV
$p_{T\pi}$	> 250 MeV
π Track χ^2/dof	< 4
π Minimum IP- χ^2 w.r.t. PV	> 10
p_μ	> 3000 MeV
$p_{T\mu}$	> 250 MeV
μ Track χ^2/dof	< 4
μ Minimum IP- χ^2 w.r.t. PV	> 12
μ Ghost probability	< 0.5
μ PID _K	< 0
μ PID _p	< 0
μ PID _{μ}	> 0

At the second level of HLT2, shown in Table 7.3, we place requirements on all three tracks, and require large enough momenta, large impact parameters and good particle identification. On top, we also reconstruct the B and HNL candidates, which we require to have good enough vertex and track quality, a fitting mass, and that the HNL vertex is well-separated from the PV.

Table 7.4: Offline trigger selection.

Trigger decision	Cut	Value
Stripping	$(N \text{ Vertex} - B \text{ Vertex})$	$> -1 \text{ mm (SS)}$
	$(N \text{ Vertex} - B \text{ Vertex})$	$> 5 \text{ mm (OS)}$
	GEC nTracks	< 300
Preselection	$N \text{ Vertex } \chi^2/\text{dof}$	< 8
	$\pi \text{ isMuon}$	$= 0$
	$\pi \text{ inMuonAcc}$	$= 1$
	$\pi \text{ ProbNNpi}$	> 0.05
	$\mu \text{ Ghost probability}$	< 0.35

Stripping and preselection are described in Table 7.4. In stripping, we place a requirement on the displacement of the N and B vertex for OS muons because the SM background is much larger for OS muons, as described in section 5.1, as well as another general cut on track number, to reduce combinatorics.

Finally, in the preselection, we place a stronger requirement on the N -Vertex fit, as well as require that the pion is in the muon acceptance and that it is not identified as a muon. We also require that ProbNN (a neural net measure that calculates a probability for a particle to actually be the the particle it is identified as, based on track fits) triggers on the muon, and a low muon ghost probability.

8 Corrected Mass Technique

In this chapter we discuss the reconstruction of the HNL mass. Looking at the inclusive decay as described in chapter 5, we will have unreconstructed particles in all inclusive final states. The only particles we can properly reconstruct in the final state is the $\mu\pi$ system. We therefore neglect the other products of the HNL decay and reconstruct them using the corrected mass approach [2] described in this chapter. This will give us a lower bound for the HNL mass.

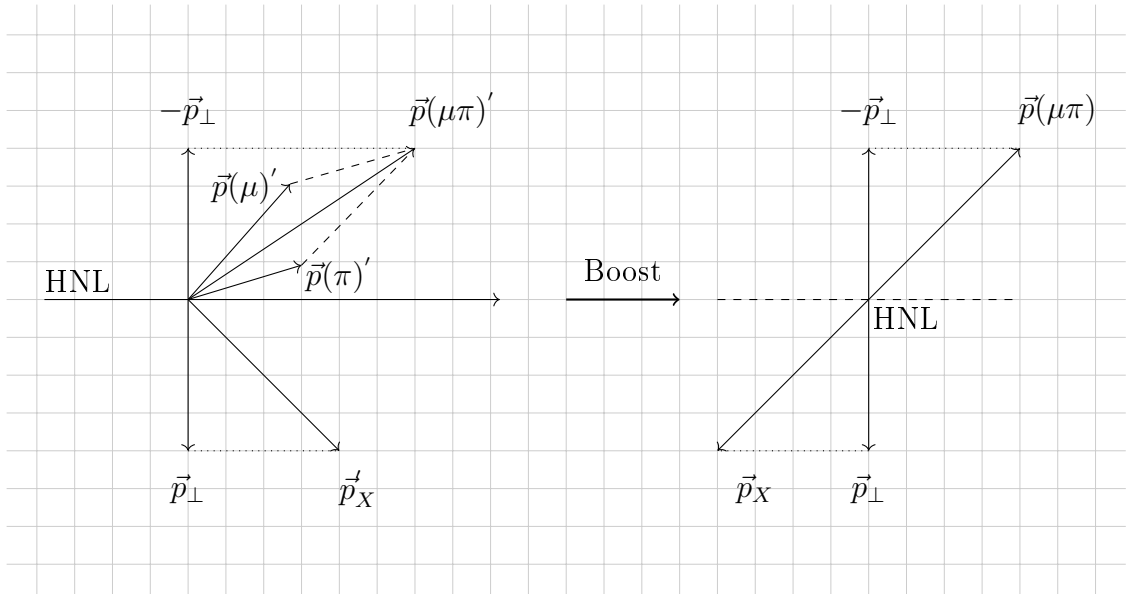


Figure 8.1: Schematic of the corrected mass approach. We boost to the HNL mass frame to be able to drop its momentum in the following calculations.

The decay products of the HNL will be a muon-pion pair and a third particle X . We measure a muon-pion pair and miss a particle we will call X . Looking at the decay of these two products in the HNL rest frame ($p = 0$), we can calculate the HNL mass as shown in Equation 8.1.

$$\begin{aligned}
 M_{\text{HNL}} &= \sqrt{E_{\text{HNL}}^2 - p_{\text{HNL}}^2} = E_{\text{HNL}} = E_{\text{vis}} + E_X \\
 &= \sqrt{m_{\text{vis}}^2 + p_{\text{vis}}^2} + \sqrt{m_X^2 + p_X^2} \\
 &= \sqrt{m_{\text{vis}}^2 + p_{\text{vis}\perp}^2 + p_{\text{vis}\parallel}^2} + \sqrt{m_X^2 + p_{X\perp}^2 + p_{X\parallel}^2} \quad (8.1)
 \end{aligned}$$

Here, E_{vis} , m_{vis} and p_{vis} denote the energy, mass and momentum of the muon-pion pair, and E_X , m_X and p_X denote energy, mass and momentum of the missing par-

ticle or particles respectively. We can split both momenta into their parallel and perpendicular components with respect to the HNL flight direction.

By conservation of momentum, we can equate $p_{\text{vis}\perp} = p_{X\perp} = p_{\perp}$, as shown in Figure 8.1. Now we can obtain a lower bound on the HNL mass by dropping the momentum parallel to the HNL flight direction in both the $\mu\pi$ and the missing particle system. We drop the parallel momentum because we cannot calculate it. The boost of the HNL is unknown, and while the perpendicular momentum does not depend on it, the parallel momentum does.

$$\begin{aligned}
 M_{\text{HNL}} &> \sqrt{m_{\text{vis}}^2 + p_{\perp}^2} + \sqrt{m_X^2 + p_{\perp}^2} \\
 M_{\text{HNL}} &> \sqrt{m_{\text{vis}}^2 + p_{\perp}^2} + p_{\perp} \quad \text{if } m_X^2 \ll p_{\perp}^2
 \end{aligned}
 \tag{8.2}$$

Here, p_{\perp} is the momentum component of both $p(\mu\pi)$ and p_X perpendicular to the flight direction of the HNL and m_{vis} is the invariant mass of the $\mu\pi$ system. Simulation shows that the mass peaks quite well with this technique, even though dropping the mass term is not necessarily appropriate for larger neutral particles.

We use the pp vertex instead of the B^0 vertex to reconstruct the corrected mass as well, because large displacements of the HNL decay vertex and the fact that we only reconstruct the μ from the B^0 , but the $\mu\pi$ system from the HNL substantially deteriorates the resolution on the position of the B^0 vertex.

This effect can be seen in Figure 8.3, where using the reconstructed B^0 vertex (turquoise) to reconstruct the corrected mass leads to an asymmetric distribution, where the HNL mass is underestimated and we get sparingly little events above the true HNL mass. Using the true B^0 vertex (orange) for the reconstruction gives us a nicer peak, but since we do not have this to make use of in real data, using the pp vertex is the best choice. We can see that using the pp vertex (blue) overestimates the HNL mass in comparison to the true B vertex, an effect that seen more clearly in Figure 8.4. A visualisation of this can be seen in Figure 8.2.

Putting both the underestimation because of the missing momentum and the overestimation through use of the pp vertex together gives us a nice symmetrical resonance, even if this does not agree perfectly with the true HNL mass distribution, which has a less broad tail towards higher masses.

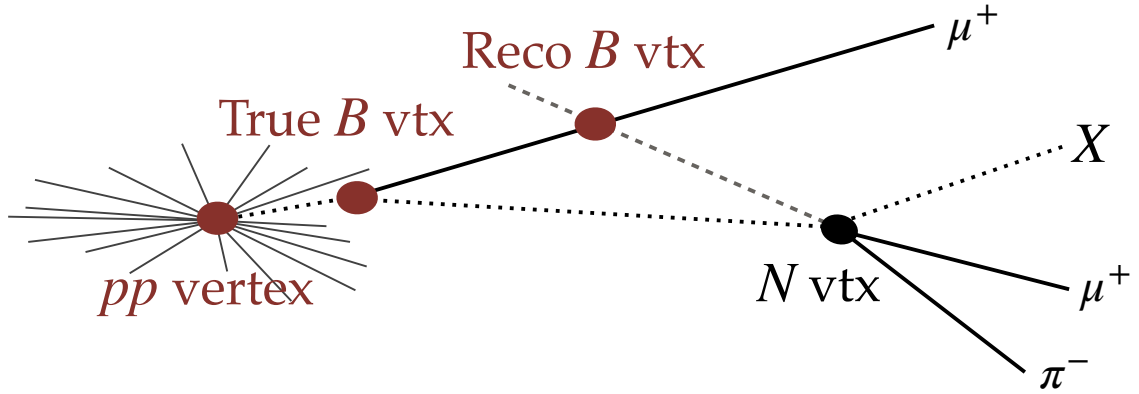


Figure 8.2: Schematic showing the difference between the pp vertex, the true B vertex and the reconstructed B vertex. The latter is poorly reconstructed since we only reconstruct it from one muon and the interpolated flight direction of the HNL, reconstructed from the $\pi\mu$ system.

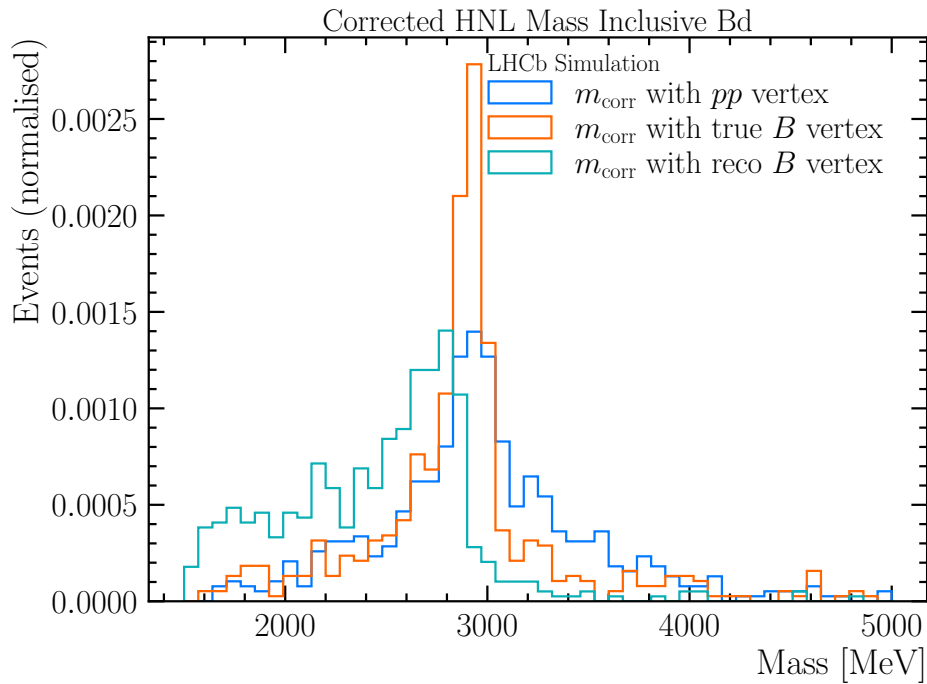


Figure 8.3: Comparison of reconstructing the HNL mass via the true B vertex, the reconstructed B vertex or the pp vertex.

We will now look at both the exclusive and inclusive decay channel and compare how the HNL mass peaks with and without the corrected mass technique. Both of these samples produce the HNL inclusively. Note that here we are going to look at the exclusive HNL decay channel $N \rightarrow \mu\pi$ versus the inclusive channel $N \rightarrow X\mu\pi$, where the inclusive sample does not contain the exclusive one. The samples here

are produced with $M_{\text{HNL}} = 3000$ MeV. The samples for the three different lifetimes of (10, 100 and 1000) ps are merged together.

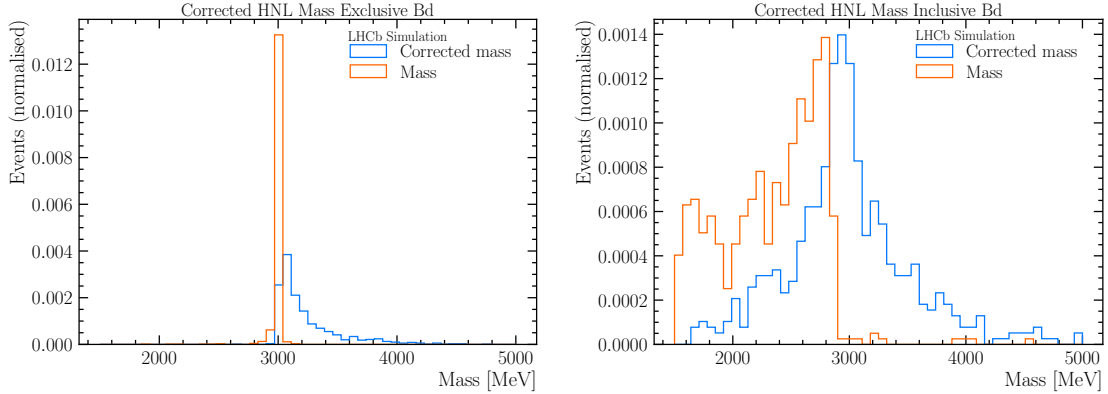


Figure 8.4: Corrected mass vs $\mu\pi$ invariant mass plot inclusive and exclusive MC. Both histograms show the invariant mass of the HNL, on the left for the exclusive channel and for the inclusive channel on the right. We see that for the inclusive channel we underestimate the true HNL mass and need to correct for the missing momentum as explained above.

The mass distributions behave as expected. For the exclusive sample, that does not include any missing particles, we slightly statistically overestimate the HNL mass because we are using the pp vertex instead of the B^0 vertex to reconstruct the flight direction of the HNL. This means the flight direction of the HNL is not perfectly reconstructed, which leads to the alignment with the $\mu\pi$ system being slightly off. This effect does not stem from the corrected mass formula itself, since we do not have any missing particles to correct for in the exclusive decay channel.

For the inclusive decay channel that will often have a missing particle, we see that the the normal mass distribution does not peak well and underestimates the mass quite significantly. Correcting with Equation 8.2 gives us a nice peak at the generated mass of $M_{\text{HNL}} = 3000$ MeV.

We now want to examine the dependence of the mass as well as the resolution of the mass peak on the displacement of the HNL from the B^0 (or in our case the pp) vertex. To do this, the displacement was binned in five bins with equal statistics, and for each the median of the distribution and the resolution of the mass peak were determined. In Figure 8.5 we can see that the simulated mass calculated with the corrected mass technique is quite close to the true mass of the HNL, but does not change a lot with the displacement, except for a slight downwards trend. There are a few outliers, but in general the mass agrees quite well with the true mass, a little less so for large displacements.

For the resolution, shown in Figure 8.6 of the mass peak, things look different,

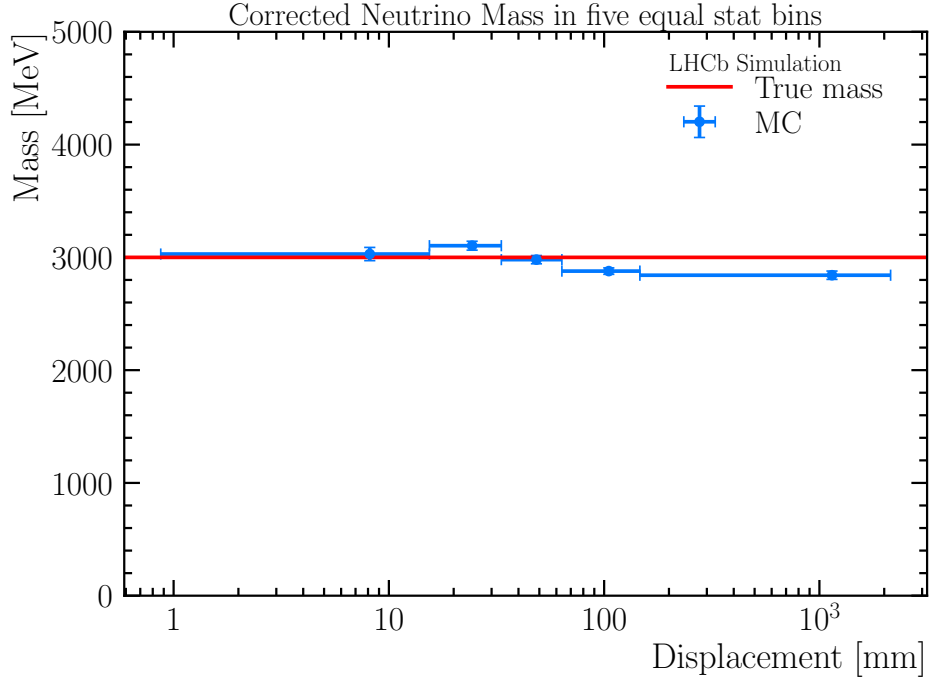


Figure 8.5: Displacement vs mass, calculated via the median of the MC in the corresponding bin. Histograms of each bins mass distribution can be found in Appendix A.

here we see a strong correlation between the width of the peak and the displacement of the HNL. This is mainly because we are using the pp vertex to reconstruct the HNL flight direction. The shorter the displacement, the larger the error on the flight direction will be, leaving us with statistically more frequent wrong reconstructions and therefore a wider HNL mass peak.

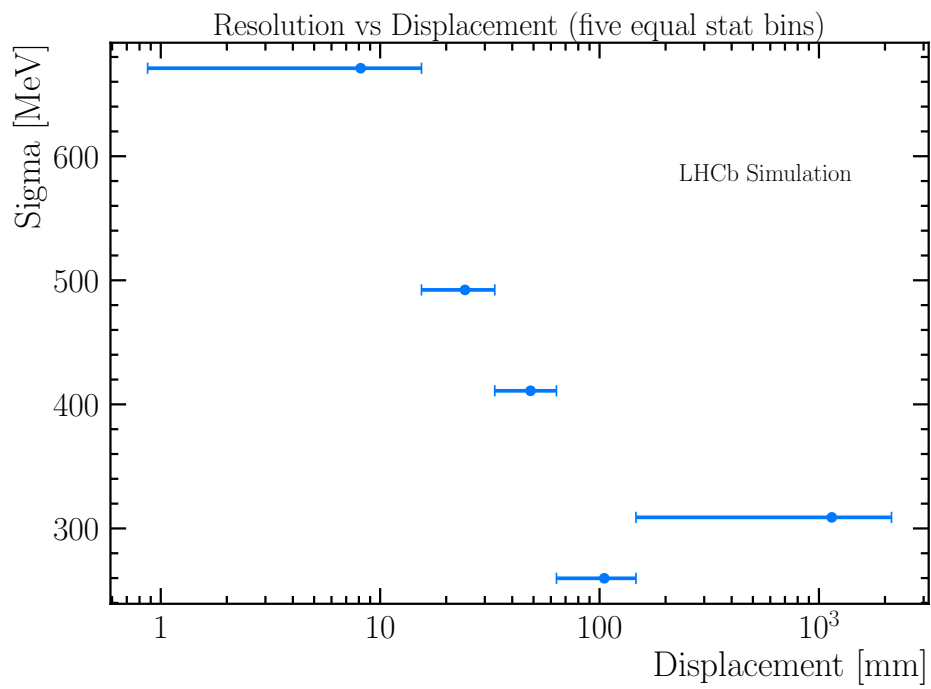


Figure 8.6: Displacement vs mass peak resolution, calculated as the average of the 1σ quantiles around the median.

9 Event rate ratio

Lastly, we want to look at the ratio of inclusively vs exclusively decayed events in correlation with the displacement of the HNL. Again, we will be using the inclusive production channel, and differentiating between the exclusive and inclusive decay of the HNL. This measure is interesting because we want to see how much statistics we gained through the inclusive channels, so it makes sense to look at the ratio of generated events after selection.

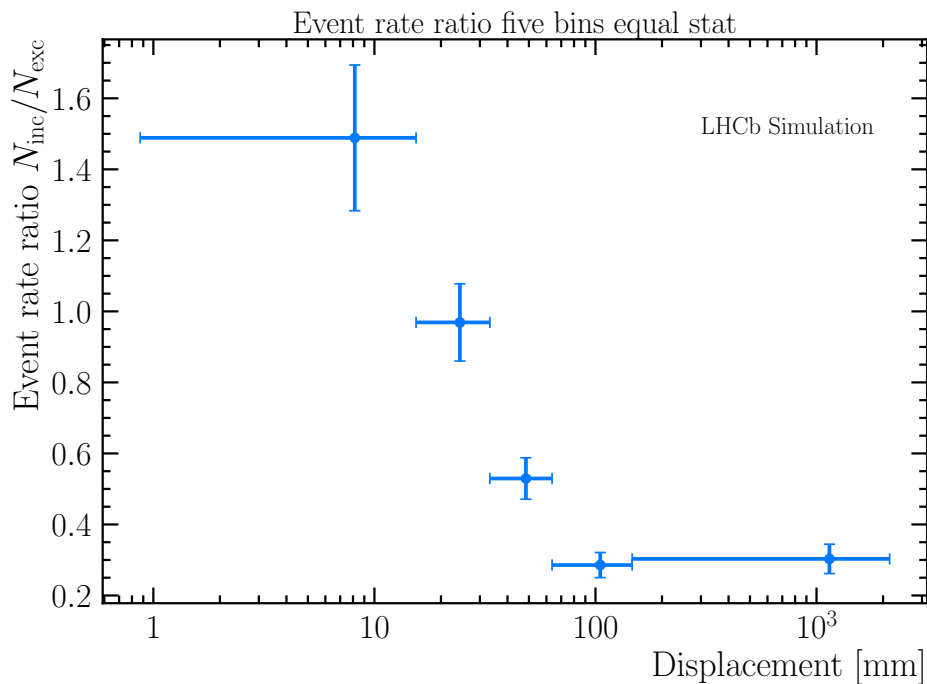


Figure 9.1: Displacement vs event rate ratio inclusive vs exclusive MC.

Again we can see a rather strong correlation, for small displacements we have a lot more inclusive data than for large displacements, where the ratio drops down to just about 20%.

In the HLT2 as shown in Table 7.3, we place a rather tight cut on the B^0 Track χ^2 . This selection was developed for the inclusive production and exclusive decay of the HNL and is not optimised for the inclusive decay. We plotted the B^0 Track χ^2 against the displacement, seen in Figure 9.2, searching for a trend of larger Track χ^2 for larger displacements in the inclusive sample. Because we reconstruct the B

meson candidates from the $\mu\pi$ system as shown in Figure 8.2 and are looking at large displacements, we expect the reconstructed B vertex to be worse in the inclusive than in the exclusive decay. Looking at Figure 9.2, we see the expected trend of larger χ^2 for larger displacements for the inclusive decay (barring an outlier in the first bin), which possibly means that we are missing quite a lot of events through this cut.

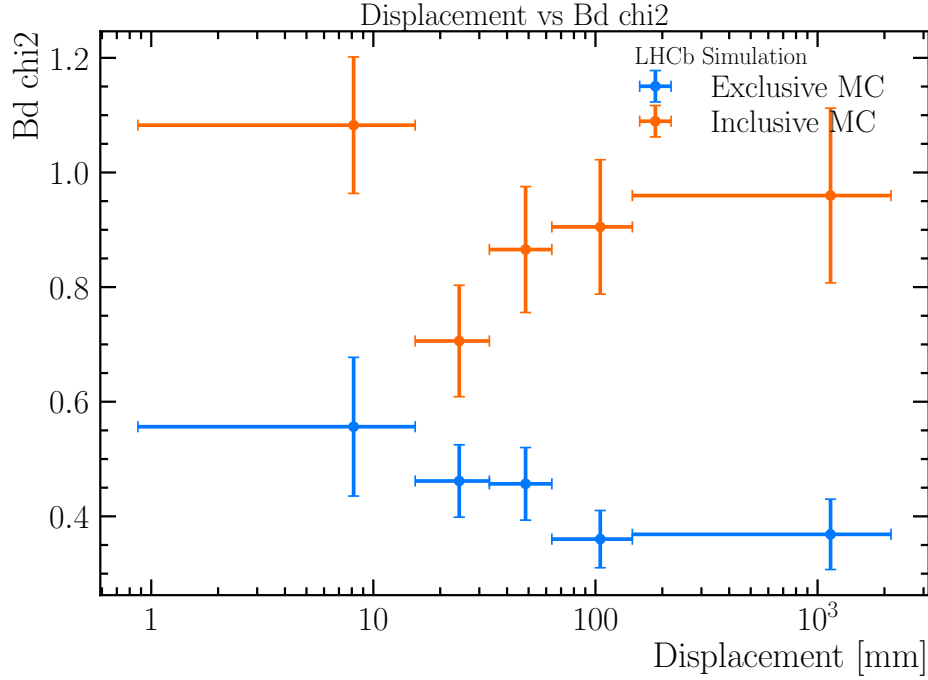


Figure 9.2: Displacement vs $B^0 \chi^2$ inclusive vs exclusive MC. Extended plots of the distribution of the χ^2 for each displacement bin can be found in Appendix B.

This issue will have to be investigated further outside the scope of this thesis. A new selection will have to be developed that takes into account the specifications of the inclusive decay channel.

Part IV

Conclusion

10 Comments and Outlook

The main work of this thesis is the setup of the production of Monte Carlo data for the production of Heavy Neutral Leptons (HNLs) from B mesons, where we both use the fully inclusive production mode of all B hadron channels, and also the inclusive decay modes. Monte Carlo data was simulated at five HNL mass points in the range of $(1.6 - 5.5)$ GeV, at three different lifetimes of $(10, 100$ and $1000)$ ps and for same sign as well as opposite sign muons in the decay.

This Monte Carlo simulation is especially important since it is not only used for the study of the fully inclusive channels, but also for the ongoing analysis of the inclusive production and exclusive decay. Furthermore the thesis provides a preliminary analysis to verify the integrity of the produced simulation. It is presented using three samples of B^0 meson decays with a Heavy Neutral Lepton mass of $m_{\text{HNL}} = 3000$ MeV, with same sign muons and three different lifetimes, $(10, 100$ and $1000)$ ps, respectively.

The fully inclusive channel is particularly interesting because it provides higher statistics to potentially significantly improve the sensitivity of the HNL search at LHCb. The drawback of the more inclusive approach is larger backgrounds contributions, which have to be studied and an appropriate selection of the data has to be developed to reduce them as much as possible while still retaining proper signal quality.

The invariant mass of the HNL is an important variable to separate signal and background and determine the signal yield in the analysis. We validate an approach to compute a corrected mass to compensate for the momenta of the missing particles in the reconstruction of the final state.

This thesis is a crucial step towards the evaluation of the sensitivity of HNL searches for LHCb. The generated Monte Carlo samples will be used by the Heidelberg LHCb group to continue this study.

Part V
Appendix

A Additional mass plots

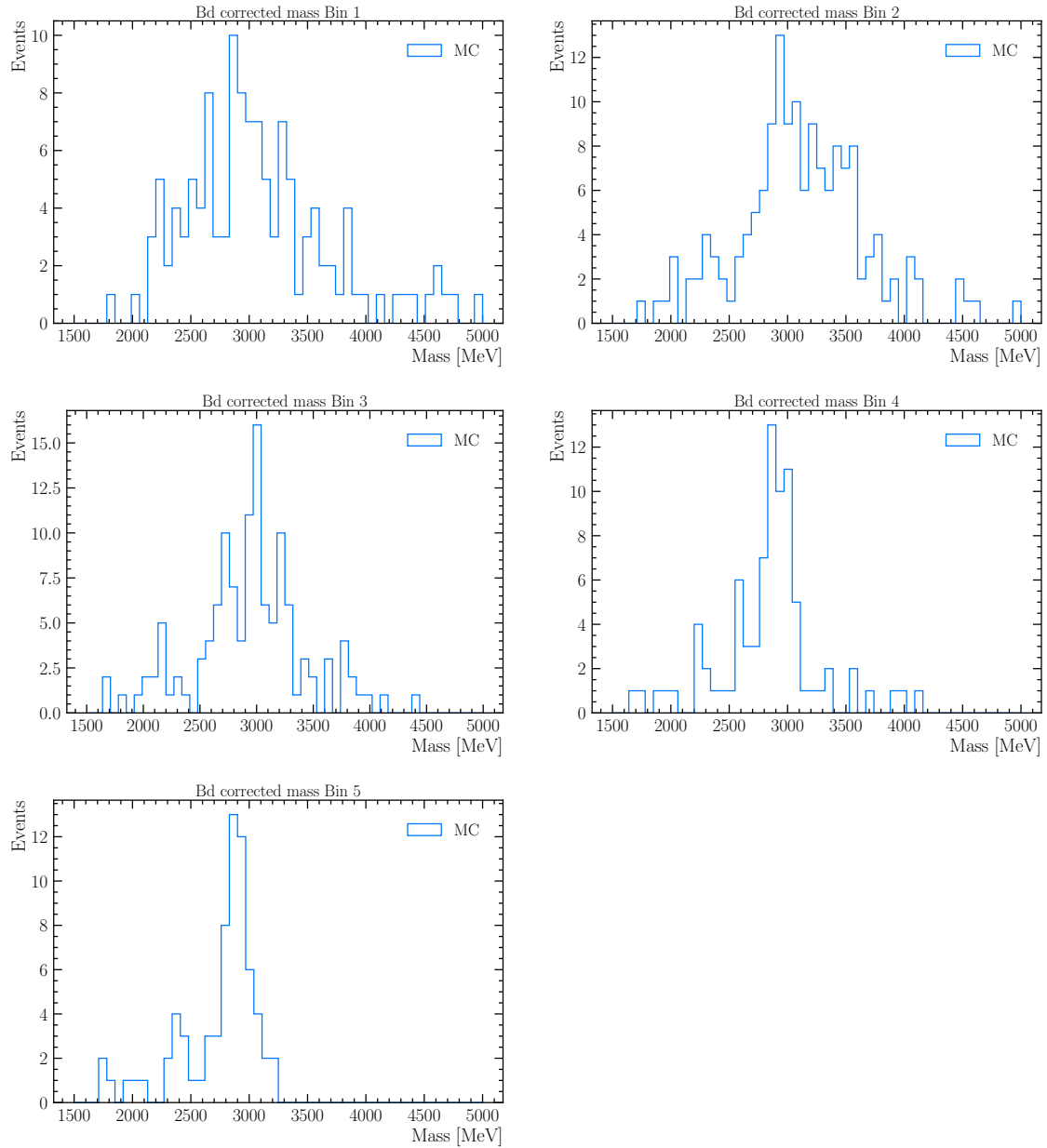


Figure A.1: B^0 corrected mass in five displacement bins with equal statistics, displacement larger the larger the binnumber. We can see that the peak gets sharper for larger displacements.

B Additional χ^2 plots

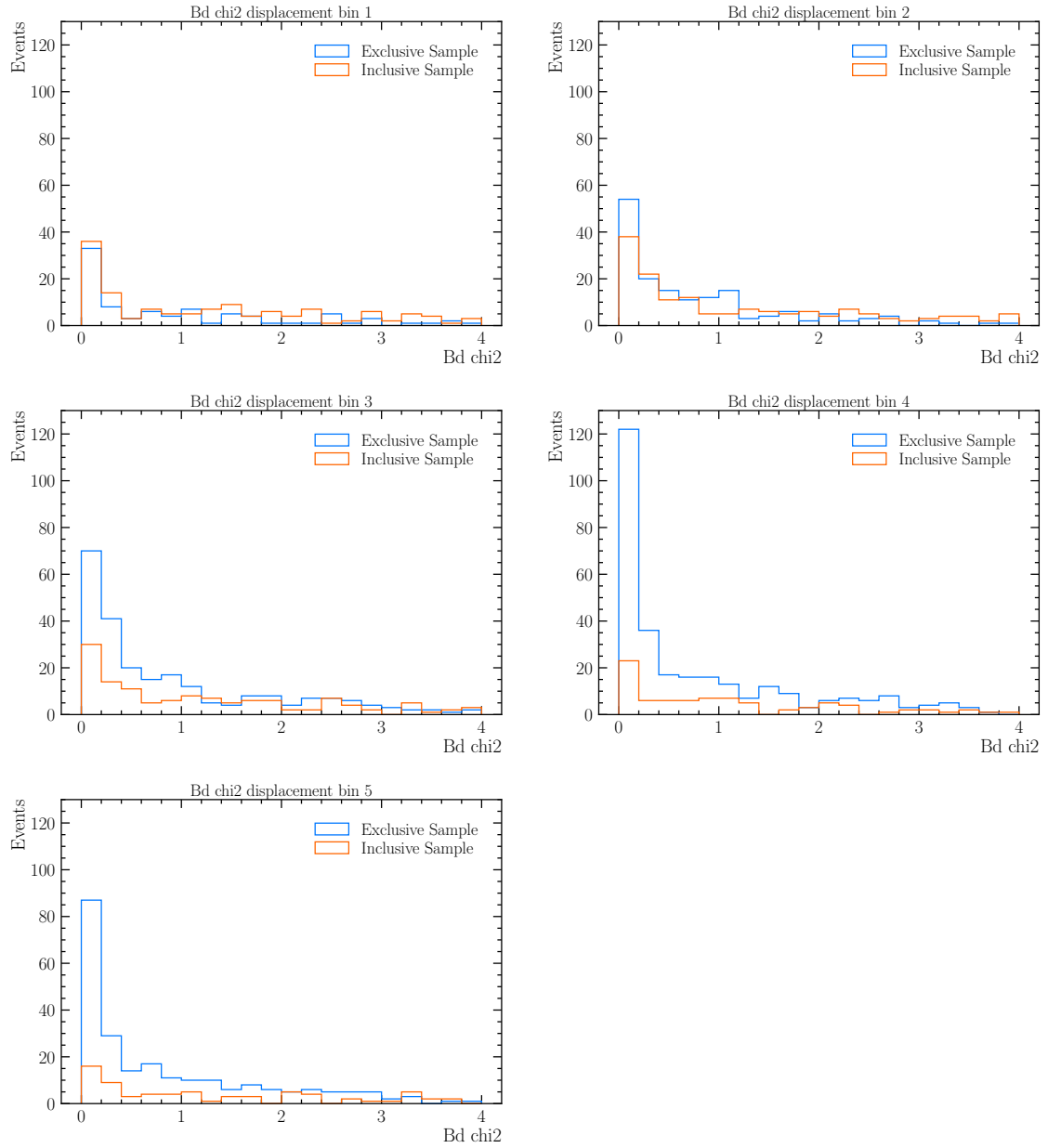


Figure B.1: $B^0 \chi^2$ histograms for each of the five displacement bins.

C Lists

C.1 List of Figures

2.1	Schematic of the LHCb detector [3].	5
2.2	Data flow at LHCb [8].	6
3.1	Elementary particles in the SM [10].	8
5.1	Feynman diagram of the exclusive production and exclusive decay of HNL.	12
5.2	Feynman diagram of the inclusive production and inclusive decay of HNL.	13
5.3	CL-exclusion region	14
5.4	B branching ratios and inclusive production sensitivity.	15
5.5	Branching ratios of the different HNL decay modes. We will not be studying the $N \rightarrow \mu^- \mu^+ \nu_\mu$ and $N \rightarrow \mu^- e^+ \nu_e$, since they are hard to detect, but it is obvious that the inclusive channel gives us a lot more statistics, especially in the higher mass regions.	16
8.1	Schematic of the corrected mass approach.	24
8.2	Schematic of vertices in decay	26
8.3	Comparison of reconstructing the HNL mass via the true B vertex, the reconstructed B vertex or the pp vertex.	26
8.4	Corrected mass vs $\mu\pi$ invariant mass plot inclusive and exclusive MC.	27
8.5	Displacement vs mass, calculated via the median of the MC in the corresponding bin.	28
8.6	Displacement vs mass peak resolution, calculated as the average of the 1σ quantiles around the median.	29
9.1	Displacement vs event rate ratio inclusive vs exclusive MC.	30
9.2	Displacement vs $B^0 \chi^2$ inclusive vs exclusive MC.	31
A.1	B^0 corrected mass in five displacement bins with equal statistics, displacement larger the larger the binnumber. We can see that the peak gets sharper for larger displacements.	35
B.1	$B^0 \chi^2$ histograms for each of the five displacement bins.	36

C.2 List of Tables

3.1	Different mesons that appear in beauty decays, their quark content and mass as well as mean lifetimes (charge conjugates are implied)[15].	9
5.1	Different production and decay modes for the HNL in beauty decays.	16
6.1	B mesons, muon signs, HNL masspoints and HNL lifetimes we want to simulate Monte Carlo data at.	18
6.2	B^0 decay branching ratios	19
6.3	HNL decay branching ratios	19
7.1	L0 trigger selection.	21
7.2	HLT1 trigger selection (Hlt1TrackMuon).	21
7.3	HLT2 trigger selection (Hlt2MajoranaBLambdaMu).	22
7.4	Offline trigger selection.	23

D Bibliography

- ¹R. Aaij, “Search for Majorana Neutrinos in $B^- \rightarrow \pi^+ \mu^- \mu^-$ Decays”, *Phys. Rev. Lett.*, **10.1103/PhysRevLett.112.131802** (2014).
- ²K. Abe et al., “Measurement of the b-quark fragmentation function in Z^0 decays”, *Phys. Rev. D - Part. Fields, Gravit. Cosmol.* **65**, 920061–9200612 (2002).
- ³A. A. Alves Jr. et al. (LHCb collaboration), “The LHCb detector at the LHC”, *JINST* **3**, S08005 (2008).
- ⁴I. Boiarska et al., “Probing baryon asymmetry of the Universe at LHC and SHiP”, **1–10** (2019).
- ⁵K. Bondarenko, A. Boyarsky, D. Gorbunov, and O. Ruchayskiy, “Phenomenology of GeV-scale heavy neutral leptons”, *J. High Energy Phys.*, **10.1007/JHEP11(2018)032** (2018).
- ⁶S. Bouchiba, “Master thesis Crafting a physics-level simulation of inclusively produced Heavy Neutral Leptons from B mesons”, PhD thesis (EPFL, 2019).
- ⁷C. H. Chang, C. Driouichi, P. Eerola, and X. G. Wu, “BCVEGPY: An event generator for hadronic production of the B_c meson”, *Comput. Phys. Commun.* **159**, 192–224 (2004).
- ⁸L. Collaboration, The LHCb Starterkit lessons, 2018.
- ⁹G. A. Cowan, D. C. Craik, and M. D. Needham, “RapidSim: An application for the fast simulation of heavy-quark hadron decays”, *Comput. Phys. Commun.* **214**, 239–246 (2017).
- ¹⁰MissMJ and Cush, Standard Model of Particle Physics, 2019.
- ¹¹A. Ryd et al., EvtGen A Monte Carlo Generator for B-Physics, tech. rep. (2004).
- ¹²T. Sjöstrand, S. Mrenna, and P. Skands, “A brief introduction to PYTHIA 8.1”, *Comput. Phys. Commun.*, **10.1016/j.cpc.2008.01.036** (2008).
- ¹³T. Sjöstrand, S. Mrenna, and P. Skands, PYTHIA 6.4 physics and manual, 2006.
- ¹⁴F. A. Thiele, chNLdecay: Calculate decay widths of Heavy Neutral Leptons, 2018.
- ¹⁵P. A. Zyla et al., Review of particle physics, 2020.

Erklärung:

Ich versichere, dass ich diese Arbeit selbstständig verfasst habe und keine anderen als die angegebenen Quellen und Hilfsmittel benutzt habe.

Heidelberg, den (Datum) 29.01.2021 *Hummel*